Chapter VI. Discussion

VI.1. THERMODYNAMIC STUDIES OF PHOSPHOLIPID MONOLAYERS

VI.1.1. Results at a temperature of 24 ºC

The features of the isotherms of pure POPE and POPC monolayers are consistent with references published elsewhere [Brockman et al., 2003; Miñones Jr. et al., 2003]. Mixed monolayers with $\chi_{POPC} \leq 0.6$ show lower areas per molecule than pure POPE, which suggests that POPC molecules can intercalate between POPE phospholipid molecules. It has been reported that the water molecules beneath the monolayer are able to form hydrogen bonds with the POPE headgroup. Additionally, PEs may form intermolecular bonds with neighbouring PEs, which creates a type of two-dimensional network at the phospholipid-water interface [Kell, 1979]. Since PC does not form hydrogen bonds, its presence in the film will interfere with the network formation [Wrigglesworth, 1995] and leads to a more favourable interaction between the hydrophobic acyl chains of the phospholipids. Therefore, the breakdown of the hydrogen bonding may be responsible for the effective decrease of the mean area per molecule, as calculated from the experimental isotherms (see Figure 47). The dynamics of formation of a hydrogen bond between a water molecule and biological entities (i.e. micelles, lipid vesicles, bilayers or proteins) is slow [Balasubramanian et al., 2002]; that is, the lifetime of the hydrogen bond established between the polar groups of the molecules of these entities and a water molecule is much longer than that between two water molecules. This implies that the PE molecules in the film are less dynamic than the PC molecules, so the attractive interactions between hydrocarbon chains could be less favoured. These observations are consistent with the differences between PC and PE headgroups reported elsewhere [Dill and Stigter, 1977].

The collapse surface pressures of mixed monolayers do not show a linear relationship between pure phospholipids, which suggests that a certain degree of immiscibility could

exist between POPE and POPC. It also seems that the miscibility between POPE and POPC molecules is correlated to the disappearance of the POPE transition when POPC is progressively introduced into the mixtures.

POPE-POPC mixtures have negative A^E values for 80% of the range of compositions and for the entire surface pressure range studied, which suggests that the predominant forces between adjacent molecules are attractive forces. These attractive forces confine the phospholipid molecules to a smaller molecular area than that observed in pure monolayers. In this analysis the A^E values are far from those required for ideal behaviour, which suggests that no phase separation exists between POPE and POPC phospholipid molecules. For $\chi_{POPC} > 0.8$, the A^E values are almost zero, which indicates ideal behaviour. A^E values calculated at a surface pressure above 30-40 $mN \cdot m^{-1}$ must be analyzed carefully because at this surface pressure some of the monolayers reach the transition point. Molecules in the different monolayers are not in the same physical state and the evaluation of miscibility can be affected.

Values of $\Delta_{mix}G$ are all negative, which suggests that no phase separation occurs in the mixed monolayers. A minimum of $\Delta_{mix}G$ is found when $\chi_{POPC} = 0.4$ for the entire range of surface pressures studied (5-40 $mN \cdot m^{-1}$) and absolute values of $\Delta_{mix}G$ increase as surface pressure increases. This behaviour is expected due to the shorter intermolecular distances reached at high surface pressures [Gong et al., 2002].

The above thermodynamic analysis indicates that the interaction between POPE and POPC is energetically favourable, showing a greater stability of the mixture in the entire range of surface pressures studied. Interestingly, many biological membranes [Marsh, 1990] and compositions used in the reconstitution of transmembrane proteins in proteoliposomes contain a high proportion of POPE [LeCoutre et al., 1997; Vázquez-Ibar et al., 2002].

Isotherms of pure POPC, pure CL and mixtures are always in the LE phase at working temperature. The area per molecule of mixed monolayers increases with the progressive addition of CL to the mixture. At 24 ºC, collapse surface pressures show a linear relationship between the two pure phospholipids, which can be interpreted as a sign of

complete miscibility between POPC and CL at the air-water interface according to the Gibbs phase rule.

The A^E values for POPC and CL mixtures are negative for all compositions and surface pressures studied. Negative A^E values indicate that the area occupied by phospholipid molecules in the mixtures is less than that attributed to an ideal mixture, which suggests that attractive forces predominate between POPC and CL molecules. From the analysis of A^E values it can be seen that a minimum is observed when χ_{CL} = 0.4 and the attractive forces between molecules are stronger. Interestingly, at high CL molar fractions ($\chi_{CL} \geq 0.8$) the A^E values tend to zero, which indicates ideal mixing properties. This effect is independent of the applied surface pressure. At a constant CL molar fraction, higher absolute values of A^E are observed at low surface pressures. This effect can be understood if we consider that when CL surface concentration is increased, due either to lateral compression or to the increase in the molar fraction of the mixture, repulsive forces between the negatively charged CL molecules counteract the attractive forces and decrease the absolute A^E values. However, proportions of POPC as low as 20% would reduce the frequency of these encounters between CL molecules and stabilize the monolayer.

Monolayer stability can be inferred from the analysis of $\Delta_{mix}G$. For POPC and CL mixtures the values of $\Delta_{mix}G$ are negative for all CL molar fractions and the entire range of surface pressures. Negative $\Delta_{mix}G$ values indicate that molecules show neither ideal behaviour nor phase separation and also suggest that the predominant forces between molecules in the monolayer are attractive. These attractive forces link molecules in a closed configuration, which creates a more stable monolayer. As in the A^E analysis, a minimum value of $\Delta_{mix}G$ exists when χ_{CL} = 0.4 and at any surface pressure, which indicates that it is the most stable mixed monolayer assayed of this two pure phospholipids. Interestingly, lower absolute values of $\Delta_{mix}G$ are found at higher surface pressures. This decrease in the stability of the monolayer may be attributed to the proximity of CL molecules. Repulsion between CL molecules that are closely compacted decreases the attractive forces that give the monolayer stability.

Importantly, we found that the value of the CL molar ratio for the more stable mixture is higher than that found in the natural mitochondrial inner membrane (χ_{CL} = 0.4) [Fleisher et al., 1967]. These results are similar to those obtained for the egg PC and CL mixture [Nichols-Smith et al., 2004], which underlines the fact that natural species have a definite influence on CL mixing properties, distribution and ultimately on the potential formation of domains.

Isotherms of pure CL and mixed monolayers are in the LE phase while POPE showed a transition, which is observed at 36.0 $mN \cdot m^{-1}$ and has been identified in the literature as an LC-LC' transition [Rey Gómez-Serranillos et al., 2004]. As stated in the Results section, POPE is the only pure monolayer which registers the transition at 24 ºC; if this is disregarded, the collapse surface pressures of mixtures decrease monotonically as the CL molar fraction is increased. This confirms the existence of ideal mixing behaviour in monolayers when $\chi_{CL} \geq 0.2$.

POPE and CL mixed monolayers have different A^E values according to surface pressure and CL molar fraction. At a surface pressure of 40 $mN \cdot m^{-1}$, the values of A^E are randomly distributed close to the dotted line that represents the ideal behaviour. This can be explained in two ways: either, molecules in the monolayers at 40 $mN \cdot m^{-1}$ mix ideally or, at this surface pressure, the two phospholipids are completely segregated in lateral enriched regions of each compound or domain. Negative A^E values can be found at $\chi_{CL} \leq 0.6$, while positive values are found at $\chi_{CL} \geq 0.8$. This behaviour can be understood, as in previous sections, if we consider that CL molecules at a high CL molar fraction can interact with each other and create repulsive forces between molecules. These repulsive forces can counteract the attractive forces between molecules, which causes a decrease in absolute values of A^E and, more importantly, produces positive A^E values. An absolute minimum value can be found at χ_{CL} = 0.2, which indicates that attractive forces action between molecules are optimum.

It is interesting to note the cross point at which the tendency of A^E values changes as a function of surface pressure, which can be seen from the different sign of $dA^E/d\pi$. Below this point ($\chi_{CL} < 0.5$) $dA^E/d\pi$ is positive and A^E values increase as the surface

pressure increases. Above the cross point ($\chi_{CL} > 0.5$) $dA^E/d\pi$ is negative and A^E values decrease as the surface pressure increases. Below the cross point, with low CL concentrations and at low surface pressures, the molecules are far away from their neighbours and CL concentration is not high enough to exert repulsion between molecules. When the surface pressure increases, the steric effect becomes stronger and generates repulsion. The proximity between CL molecules is now sufficient to produce the repulsive electrostatic interactions. Above the cross point, with a higher CL concentration and at low surface pressures, the molecules are randomly distributed over a large surface area and CL molecules can interact with each other to create repulsive forces. When lateral compression increases the surface pressure, the CL molecules compacted but POPE molecules can act as spacers that decrease the repulsion interaction between anionic molecules.

Values of $\Delta_{mix}G$ are all negative but at $\chi_{CL} = 0.8$ they tend to zero. Negative $\Delta_{mix}G$ values are indicative of attractive forces between molecules. At high values of CL molar fraction the repulsion between CL molecules counteracts this attraction and decreases the absolute values of $\Delta_{mix}G$. As in the case of A^E values, a minimum $\Delta_{mix}G$ value can be found at $\chi_{CL} = 0.2$, which indicates that this is the most thermodynamically stable monolayer of those assayed with these two phospholipids. In such a case, a new cross point appears at $\chi_{CL} \sim 0.7$, which is more enriched in CL than the cross point found in the A^E analysis. At $\chi_{CL} < 0.7$, the absolute values of $\Delta_{mix}G$ increase when the surface pressure increases, while above the cross point ($\chi_{CL} > 0.7$) the absolute values of $\Delta_{mix}G$ decrease when the surface pressure increases. At $\chi_{CL} < 0.7$, if POPE and CL molecules are not uniformly distributed, the phospholipid molecules, in particular POPE molecules, can form hydrogen bonds at low surface pressures that are broken when the increase of the surface pressure compacts the molecules. The breakdown of these hydrogen bonds can generate a new surface area which increases the stability of the monolayer. At $\chi_{CL} > 0.7$ this effect would be lower than the repulsion generated by the negative net charge of CL. These repulsive forces cause the absolute values of $\Delta_{mix}G$ to decrease when the surface pressure increases.

Remarkably, the composition at the $\Delta_{mix}G$ minimum, POPE:CL (0.8:0.2, mol:mol), corresponds to the naturally occurring ratio of such phospholipids in the inner membrane of mitochondria.

In summary, at a constant surface pressure of 30 $mN \cdot m^{-1}$, the most stable monolayer studied at 24 ºC is POPC:CL (0.8:0.2, mol:mol), while the POPE:POPC (0.6:0.4, mol:mol) monolayer is more stable than POPE:CL (0.8:0.2, mol:mol).

VI.1.2. Results at a temperature of 37 ºC

Isotherms of pure POPE, pure POPC and mixed monolayers are all in the LE phase at this temperature and no phase transition is expected. In comparison with the same analysis performed at 24 ºC, the mixed monolayers are in between pure monolayers increasing its molecular area with the POPC enrichment. In this case it appears that the POPE molecules are unable to form stable hydrogen bonds with water. Molecular agitation due to temperature can prevent or constrain the formation of this type of bond and means that POPE molecules occupy a smaller molecular area than at 24 ºC. These observations confirm the miscibility between POPE and POPC molecules. In mixed monolayers, a linear relationship exists between the collapse surface pressures of pure components, which also confirms the miscibility between components.

A^E values exhibit different behaviour when the surface pressure increases. On the one hand, at $\chi_{POPC} \leq 0.2$ with a high POPE concentration, A^E values decrease as the surface pressure increases, which indicates that steric repulsion is higher at low surface pressures. This behaviour can be attributed to the formation of unstable hydrogen bonds between POPE molecules. These hydrogen bonds restrict the mobility of the molecules in the two-dimensional space and produce higher values of A^E values at low surface pressures. When the surface pressure is increased, the proximity between POPC and POPE molecules increases, which prevents the formation of the hydrogen bonds and decreases the A^E values. This effect is important because at low surface pressures repulsive forces predominate in the monolayer (positive A^E values), while at high surface pressures the predominant forces are attractive forces (negative A^E values). On the other hand, at $\chi_{POPC} > 0.2$ A^E values increase when the surface pressure increases,

which indicates that steric repulsion is greater at high surface pressures. This is consistent with a possible repulsion generated by POPC molecules at this temperature. At low surface pressures POPC molecules are dispersed while at higher surface pressures the high mobility of the acyl chains can generate greater repulsion between molecules due to steric processes. The behaviour of A^E values at χ_{POPC} = 0.8 is particularly interesting. At low surface pressures ($\pi \leq 15$ mN·m^{-1}) attractive forces act between the molecules in the monolayer, specifically between POPC-POPC and/or POPE-POPC pairs, while at higher surface pressures ($\pi \geq 30$ mN·m^{-1}) the predominant forces are repulsive. This can be understood if we consider that the small proportion of POPE molecules at this POPC molar fraction can stabilize the monolayer at low surface pressures, while at higher surface pressures the predominant interaction is steric repulsion, which generates repulsion between molecules.

All $\Delta_{mix}G$ values are negative, which indicates that the prevailing forces in the monolayer are attractive. As expected, lower absolute values of $\Delta_{mix}G$ are observed at high surface pressures due to steric repulsion between molecules that are confined to a minor area. At this temperature the minimum values of $\Delta_{mix}G$ are not well defined but instead fall within the range χ_{POPC} = 0.4-0.8. Interestingly, the monolayer with a value of χ_{POPC} = 0.8 does not show the same behaviour as observed with A^E values. The effect on A^E values has no correlation with the $\Delta_{mix}G$ analysis, since the difference between the highest and the lowest A^E values is only ~ 5 Å^2 at this POPC molar fraction.

Isotherms of pure POPC, pure CL and mixed monolayers are in the LE phase at this temperature and no phase transition occurs. As at 24 ºC, the mixed monolayers show large molecular areas as the CL molar fraction in the mixture increases. All mixed monolayers are between pure monolayers. The molecules are well mixed and form homogeneous monolayers. This can be deduced from the variation in the collapse surface pressure of mixed monolayers. These surface pressures are arranged in a straight line, which confirms that no phase separation occurs in POPC and CL mixtures at 37 ºC.

The analysis of A^E values can provide more information about POPC and CL miscibility. Positive A^E values at low surface pressures in the range χ_{CL} = 0.2-0.4 can be attributed to the high mobility of hydrocarbon chains in both phospholipids. At a high CL molar fraction, positive A^E values can be produced by CL-CL repulsion due to the accumulation of negatively charged molecules at the monolayer surface. Negative A^E values at surface pressures greater than 25 mN·m^{-1} in the range χ_{CL} = 0.2-0.4 can be caused by the confinement of the acyl chains to smaller areas, which decreases the steric component of the interaction. This cannot occur at higher CL molar ratios because the repulsion between CL polar heads prevents the molecules from moving closer together.

Monolayer stability is evaluated by analyzing values of $\Delta_{mix}G$. All values are negative which indicates stability for all mixed monolayers studied. For monolayers with $\chi_{CL} \geq$ 0.6, lower absolute values of $\Delta_{mix}G$ are observed as the surface pressure increases. This is consistent with the fact that CL molecules are compacted at high surface pressures. This proximity can generate a degree of repulsion between molecules due to the accumulation of negative charged molecules at the interface. Interestingly, for monolayers with $\chi_{CL} < 0.4$, the absolute values of $\Delta_{mix}G$ decrease below 25 mN·m^{-1}, whereas the opposite is observed above this surface pressure. At low surface pressures ($\pi \leq$ 25 mN·m^{-1}) steric repulsion between molecules (mainly POPC molecules) is produced, which generates repulsion in the monolayer as the surface pressure is increased. At higher surface pressures ($\pi >$ 25 mN·m^{-1}) and in a homogeneous monolayer, the proximity between CL molecules POPC molecules is higher, which reduces the steric effect that can generate POPC hydrocarbon chains at this temperature.

Isotherms of pure POPE, pure CL and mixed monolayers are in the LE phase at this temperature and no phase transition occurs. As at 24 ºC, the mixed monolayers show larger molecular areas as the CL molar fraction in the mixture increases. The mixed monolayers always show features between the pure monolayers. Interestingly, the pure POPE monolayer shows a lower area per molecule than at 24 ºC, which suggests that POPE molecules may not form hydrogen bounds as easily as at 24 ºC, or that the bonds are more unstable. As at 24 ºC, if we disregard the influence of pure POPE molecules, the collapse surface pressures of the monolayers remain confined to a straight line,

which indicates miscibility at these molar fractions. The existence of miscibility for compositions with $\chi_{CL} < 0.2$ cannot be conclusively established.

The miscibility of POPE and CL monolayers can be determined by analyzing A^E values. At this temperature all A^E values are positive. The molecules occupy higher molecular areas in the monolayer than if considered as ideal gases, which indicates that the forces acting in the monolayers are mainly repulsive. Also important here is the CL molar fraction at which the maximum value of A^E is reached: $\chi_{CL} = 0.2$. This maximum is smoothed to a wide CL molar fraction range at high surface pressures ($\pi \geq 35$ mN·m^{-1}). In all monolayers studied the values of A^E decrease as the surface pressure increases, which suggests that steric repulsion may be reduced at higher surface pressures. This can be explained by the ability of POPE to generate hydrogen bonds that stabilize the monolayer when POPE molecules are in close proximity.

The $\Delta_{mix}G$ analysis provided both positive and negative values. Negative values at low surface pressures are caused by the low interaction between molecules and the hydrogen bonding between POPE-POPE or POPE-CL molecules which may stabilize the monolayer. When the surface pressure is increased molecules interact at close range and the steric effect can destabilize the monolayer. Moreover, at higher surface pressures CL molecules are affected by repulsive forces due to an accumulation of surface charge.

VI.1.3. POPE monolayer

The so-named LC-LC' transition occurs in the POPE isotherm at 24 ºC and gradually disappears when POPC or CL molecules are added to the mixed monolayers. The same phase transition is not observed in the POPE isotherm at 37 ºC. Isotherms at different temperatures show that the LC-LC' transition completely disappears at temperatures above than 29 ºC. Interestingly, when the temperature is increased the area per molecule of the transition decreases monotonically, whereas the surface pressure increases with temperature. This is due to a change in the spatial molecular orientation caused by the increased temperature. At low temperatures, the molecules are less dynamic and the hydrogen bond between adjacent molecules creates two-dimensional structures that increase the area per molecule at the transition. When the temperature is increased, the

molecules in the monolayers gain mobility and either impede the formation of the hydrogen bonds or decrease their life time. This increased mobility allows molecules to be compacted to high surface pressures and lower areas per molecule. At 37 ºC, the absence of the LC-LC' transition suggests that the mobility of molecules in the monolayer produces lateral instability at high surface pressures, which causes the POPE monolayer to collapse before the transition can appear.

The wide peak observed in the C_s analysis provides information on the LC-LC' transition, because the value of C_s is suddenly modified at this point but subsequently returns to similar values. The LC-LC' transition extends over a wide range of surface pressures ($\Delta\pi \sim 7\text{-}10$ mN·m^{-1}). The surface pressure at the observed peak increases with temperature and the transition disappears in the monolayer at 37 ºC. It is more difficult to give a physical explanation for the second observed peak, but it can be related to the second transition observed in monolayers at $T \leq 24$ ºC. This second point can be interpreted as a transition to a more condensed phase.

V.1.4. *Cyt c* adsorption to monolayers

The CL monolayer shows the maximum value of ΔA due to *cyt c* adsorption, while the POPC and POPC:CL (0.6:0.4, mol:mol) monolayers show a similar response to *cyt c* adsorption and lower ΔA values than pure CL. Interactions between CL and *cyt c* are mainly electrostatic due to the positive charge carried by *cyt c* at pH 7.40 (pI ~ 10) and the negative charge of CL. POPC is a zwitterionic phospholipid that can adsorb *cyt c* due to hydrogen bonding or van der Waals interactions. Therefore, *cyt c* shows greater adsorption to acidic monolayers than to zwitterionic monolayers. It is interesting to consider the response of the POPC:CL(0.6:0.4, mol:mol) mixed monolayer to *cyt c* adsorption. The mixed monolayer responds similarly to pure POPC, despite the high CL proportions in the mixture. In section VI.1.1. we discuss the observation that POPC and CL molecules form well-mixed monolayers and do not show lipid segregation at 24 ºC. The results for this composition indicate that because the CL and POPC molecules are uniformly distributed in the monolayer, they do not form specific surface charge regions in which electrostatic bonds are formed with *cyt c*. It is then reasonable to conclude that *cyt c* adsorption to the POPC:CL (0.6:0.4, mol:mol) monolayer is mainly due to van der

Waals forces between the phospholipid molecules and the protein. Interestingly, the POPC:CL (0.6:0.4, mol:mol) monolayer shows consistently lower ΔA values than pure POPC. If we assume that i) phospholipid-*cyt c* interactions in the pure and mixed monolayers are mainly due to van der Waals forces and ii) pure POPC has a lower transition temperature than the mixture and therefore greater molecular mobility, then *cyt c* will be adsorbed more deeply in the POPC monolayer than in POPC:CL (0.6:0.4, mol:mol), thus increasing the area per molecule of the pure monolayer.

POPE is a zwitterionic phospholipid that can bind *cyt c* by the formation of hydrogen bonds and van der Waals interactions, although pure POPE shows lower values of ΔA than pure POPC. This can be explained by a number of factors: POPE tends to form hydrogen bonds between neighbours, which reduces the specific area to which *cyt c* can be bound; POPE has a lower area per molecule than POPC at the same surface pressure, so *cyt c* can be adsorbed easily to POPC monolayers without altering their stability; POPC shows a lower transition temperature than POPE in liposomes, which suggests that *cyt c* can be adsorbed easily to POPC. The mixed POPE:CL (0.8:0.2, mol:mol) monolayer shows mainly electrostatic interactions with *cyt c*, but van der Waals interactions are also significant due to the high proportion of the zwitterionic phospholipid present. The thermodynamic analysis of POPE and CL at 24 ºC indicates that POPE and CL can be laterally segregated in the monolayer, so POPE and CL molecules are not uniformly distributed in the monolayer. This asymmetric distribution produces specific charge regions to which *cyt c* can be electrostatically bound (CL-enriched domains) and regions to which it can be bound through van der Waals interactions (POPE-enriched domains). Although the mixed monolayer contains only 20% CL, the value of ΔA is half that of the pure CL monolayer. It is reported that *cyt c* has a specific binding site for anionic phospholipids, but that not all CL molecules in the monolayer can bind a protein. *Cyt c* has a main surface of 110 nm^2 while the area of a CL molecule, at π = 30 $mN \cdot m^{-1}$, is 2.2 nm^2. If we consider that one *cyt c* molecule is bound to a single CL molecule, then there must be an excluding monolayer surface to which no other *cyt c* molecule can be bound. From these results we can determine that the POPE:CL (0.8:0.2, mol:mol) monolayer has half the number of effective binding sites of the total for the pure CL monolayer.

VI.2. AFM LB FILM CHARACTERIZATION

LB films of pure and the most stable binary mixed monolayers as identified by the thermodynamic analysis were extracted on a well-defined, flat support, that is, mica. By viewing the monolayers with an AFM it was possible to gain information about the arrangement of molecules at the air-water interface.

Pure POPC LB films show flat, featureless monolayers on the solid support at both extraction surface pressures. This can be understood if we consider that POPC is always in both the LE [Brockman et al., 2003] and fluid phase [Hernández-Borrell and Keough, 1993] at the extraction temperature, irrespective of the surface pressure. In these cases, the topographic images of pure PCs cannot provide any relevant physical information and the AFM *per se* is very limited, meaning that different approaches are required. In this study we used fluorescence measurements of liposomes in solution.

The pure CL monolayer shows different topographic features according to the extraction surface pressures. At a surface pressure of 20 $mN \cdot m^{-1}$ the monolayer covers the entire mica surface and shows a homogeneous surface. Neither nano- nor microdomains are observed. The CL molecules appear to be randomly distributed. At a surface pressure of 30 $mN \cdot m^{-1}$, structures forming a two-dimensional channel-like distribution appear. The CL molecules are also close enough to exert stronger interactions on neighbouring molecules: i) CL molecules carry negative charge that produces electrostatic repulsion between molecules; and ii) van der Waals forces between rearranged hydrocarbon chains can generate attractive forces based on the hydrophobic effect. In this case, there is a balance between the charge repulsion and van der Waals forces because head groups are confined to the mica surface while hydrocarbon chains can move freely. Then, the hydrocarbon chains can interact strongly and decrease the tilting respect to the vertical phospholipid direction to the surface than when they are randomly distributed. The channel-like arrangement of phospholipids is caused by the fracture and reorganization of the existing monolayer at lower surface pressures.

Although POPE shows the same hydrocarbon chains as POPC, the PE head group, which is smaller than the PC group [Dill and Stiger, 1977], is responsible for the higher transition temperature in liposome suspensions (T_m ~ 25 ºC). This property may restrict the mobility of POPE at the air-water interface at 24 ºC. This should in turn be related to the formation of hydrogen bonds with the water molecules beneath the monolayers and (less conclusively) to the formation of hexagonal phases at the air-water interface [Tate et al., 1991]

Pure POPE LB films display different monomolecular structures at different surface pressures. At a surface pressure of 20 $mN \cdot m^{-1}$ the AFM image of POPE shows a homogeneous structure that covers the whole mica surface. At a surface pressure of 30 $mN \cdot m^{-1}$, the POPE LB film covers the whole substrate with a monolayer that contains a large number of round structures that pierce slightly the phospholipid layer. These round structures could show, or be a first step in, the reorganization of the molecules that leads to the so claimed LC-LC' transition [Rey Gómez-Serranillos et al., 2004] of POPE at this temperature and at higher surface pressures. It is also important to consider that the deposition of the monolayer on a solid support may modify its properties on the mica surface [Reigler and Spratte, 1992]. Furthermore, it is also possible that defects could appear even when the transfer ratio is 1. When the orientation of the POPE molecules changes from the second-neighbour to the first-neighbour molecule, free spaces are created. This effect is illustrated in the cartoon model shown in Figure 107. If this occurred simultaneously in a cooperative process, a large number of small, round structures would be expected to appear due to the homogeneity of the monolayer.

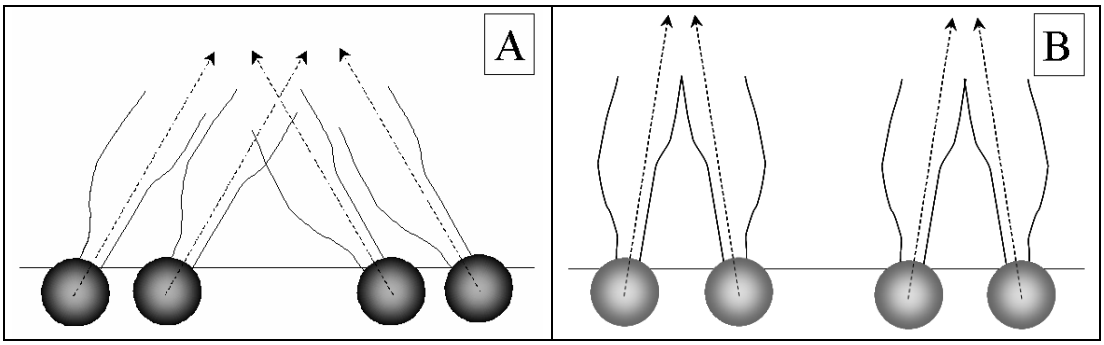

Figure 107. Phospholipids oriented towards A) second and B) first neighbours.

When the surface pressure is increased up to 30 $mN \cdot m^{-1}$, the pure POPE monolayer relaxes, which increases the diameter of the free spaces observed. This relaxation process can be caused by the fusion of small holes under lateral compaction which increases the uncovered areas. Simultaneously to this process, the compactness prevents the generation of further defects. This explains the two structures or areas that we observe in the LB film (Figure 75): one very similar to those at a surface pressure of 30 $mN \cdot m^{-1}$ but with holes or vacancies with larger diameters, and another that is taller than the first and corresponds to a more condensed material. The condensed structure is not homogeneous and displays numerous fractures or fissures on its surface. This condensed phase is formed by structures of 25 μm in diameter distributed randomly across the whole monolayer.

BAM is a technique for monitoring the optical changes in the monolayer at the air-water interface [Hénon and Méunier, 199; Hoenig and Moebius, 1991]. Images obtained with this technique contain a map of the optical reflectivity of the monolayer, which correlates with the local packing density. Denser phases appear brighter. At very low surface pressures, the POPE monolayer shows the typical gas-liquid expanded phase coexistence. The dark gas phase disappears with increasing surface pressure, which leaves a brighter, homogeneous layer that covers the entire observed region. During lateral compression, a new structure appears in the BAM images at values close to $\pi \sim 6$ $mN \cdot m^{-1}$, although there is no observable feature either in the isotherms or in the C_s analysis of the monolayer performed in section V.1.3.2. These new structures are small and bright spots that can be seen over the entire monolayer surface. Although their exact nature is unknown, the BAM images show that they are more condensed than the LE phase. Upon nucleation the structures appear blurred but they become sharper during lateral compression. This may suggest that their initial size is similar to or below BAM resolution (~ 1 μm) and that they then increase in size at higher pressures. The structures are present in the monolayer in a range of surface pressures from 6 to 45 $mN \cdot m^{-1}$ in largely constant numbers over the whole range.

The BAM images show ordering at micron length-scales and above, which should be related to the AFM observations, since these are typically used to obtain information at the nanoscopic level. These bright spots appear to be related to the formation of holes

observed in the AFM images. They may be the result of POPE molecules that show stronger lateral cohesion than others. The molecular cohesion can be caused by the formation of stronger interactions between POPE molecules or between POPE molecules and water when the phospholipid is in the LE phase. Interestingly, at a surface pressure of ~ 45 $mN \cdot m^{-1}$ a condensed phase nucleates around these spots. The sizes of the condensed domains are consistent with the structures seen in the AFM images of LB films extracted at a surface pressure of approximately 39 $mN \cdot m^{-1}$. In the AFM images these structures are not as homogeneously distributed as in the BAM images, although this could be caused during the transfer to the solid support. At this point, BAM and AFM – usually two very different techniques – act as complementary tools to reflect the same property.

Surprisingly, the expected phase transition at $\pi \sim 36$ $mN \cdot m^{-1}$, as observed in the surface pressure isotherms, does not produce any change in the BAM images. A possible explanation for this observation is that the vertical modification of the hydrocarbon chain tilt from the first to the second neighbour is undetected by the technique used here.

The behaviour of the POPE:POPC (0.6:0.4, mol:mol) LB films is more similar to that of the pure POPC monolayer than to that of the pure POPE monolayer. The mixed monolayer shows a featureless structure at both surface pressures without any vacancy but with distinguishable protrusions on its surface. POPC molecules may be positioned between POPE molecules, thus preventing the formation of holes. This is reflected in the mixed monolayers (Figure 79), in which the area per molecule is smaller than that of pure POPE.

POPC:CL (0.6:0.4, mol:mol) LB films show no distinguishing features on the surface of the monolayer but contain numerous protrusions. At a surface pressure of 20 $mN \cdot m^{-1}$, the mixed LB film is completely consistent with both pure phospholipids. However, at a surface pressure of 30 $mN \cdot m^{-1}$, the mixed LB film is more similar to pure POPC than to pure CL. This suggests that the addition of POPC molecules to a CL monolayer increases its stability and prevents the formation of ruptures. POPC molecules, as in the case of the POPE:POPC mixture, can occupy spaces between CL molecules, which

decreases repulsive interactions. As a result, the CL molecules are less strongly bound to the mica surface and have sufficient mobility to form a perfect LB film without fractures.

The POPE:CL (0.8:0.2, mol:mol) LB film at a surface pressure of 20 $mN \cdot m^{-1}$ shows similar features to pure POPE at the same surface pressure, but the structure of the mixed monolayer presents clearly defined edges. More interesting results are obtained for the LB film at a surface pressure of 30 $mN \cdot m^{-1}$. In this image different structures are clearly seen in different regions. One structure is quite similar to that of pure CL, while the other is very similar to that of pure POPE. This image can be used to corroborate the lateral segregation of the monolayer observed during the thermodynamic analysis discussed in previous sections.

The images of POPE:POPC:CL (0.5:0.3:0.2, mol:mol:mol) LB films are similar to those of pure POPC, but less protrusions are visible on the surface. This suggests that POPC molecules determine the characteristics of the LB films at both surface pressures studied. Therefore, the molecules in the LB films are in the LE phase at the extraction temperature.

VI.3. FLUORIMETRIC SURFACE STUDIES

The incorporation of *cyt c* to liposomes is investigated by measuring the variation in surface electrostatic potential produced by adding the protein to pure and mixed liposomes. As expected, the fluorescence of naked liposomes is higher than fluorescence of liposomes in which the protein is incubated. *Cyt c* has a positive net charge at pH 7.40 and competes with ANS for the binding sites in the sample. As a result of this competition, fewer ANS molecules can be bound to the liposome, which in turn decreases the fluorescence of the sample.

Fluorescence intensities are higher in POPC samples than in other compositions. This can be explained by the fact that ANS binds more readily to zwitterionic phospholipids such as POPC than to negatively charged CL or to POPE because its ability to form

intermolecular hydrogen bonds. These hydrogen bonds generate a two-dimensional network that can either interfere in the binding of the fluorescent probe or decrease the association constant of ANS to liposomes in these compositions. This can be clearly observed in Figure 87, in which pure POPC shows fluorescence intensity close to 1000 a.u., while samples containing POPE or CL show fluorescence intensities below 250 a.u. It can also be seen in Table XIV that the emission coefficient of POPC is four times greater than those of POPE or CL, which suggests that more ANS molecules bind to liposomes containing POPC than to liposomes with different compositions.

Cyt c is known to have a higher affinity for anionic phospholipids as CL or PG [Nichols, 1974]. In these types of phospholipid, the main force of the interaction with *cyt c* is electrostatic, while in zwitterionic phospholipids such as PE or PC, the protein interaction is mainly governed by non-ionic forces [Rytomaa, 1992]. This different interaction between *cyt c* and the lipids studied is demonstrated by the fluorescence analysis. The variation in fluorescence intensity due to the incorporation of *cyt c* is far greater in the CL-containing samples than in samples without CL. Interestingly, of mixed samples containing CL, the maximum fluorescence variation due to *cyt c* incorporation is observed in liposomes of POPE:CL (0.8:0.2, mol:mol), which is the composition that exhibits phase separation according to the thermodynamic analysis. Moreover, the plots show that *cyt c* interacts more strongly with POPC than with POPE. This can be clearly seen in the binding curve of pure POPE, in which the variation due to *cyt c* incorporation is almost negligible. At 24 ºC, pure POPE is close to its transition temperature, while the transition temperature of POPC is – 2 ºC. This means that POPC molecules have greater mobility than POPE molecules at working temperature. Because of this fluidity, *cyt c* molecules can bind both to the surface and to deeper positions in the liposome [Gorbenko, 1999]. In POPE liposomes, since the phospholipid is at its transition temperature and PE can form hydrogen bounds, *cyt c* can be bound only to the surface of the liposome and to a lesser degree than in POPC liposomes.

As expected, the mathematical adjustment of data obtained from blanks confirms that samples containing POPC exhibit more ANS binding than others. This can be seen from the values of k_0 in Table XV. The k_0 value of pure POPC is four times greater than that of pure POPE, while mixtures containing CL showed k_0 values of the same order. The

mathematical adjustment of data in samples containing *cyt c* can be calculated considering either one or two ANS binding sites. One binding site is for the binding of ANS to the phospholipid and the other is for possible binding of ANS to *cyt c*. The next step was to measure the effect on fluorescence of the binding of ANS to free *cyt c* in solution. Fluorescence measurements were consistently similar to the fluorescence of ANS in water, which demonstrates that ANS does not bind to free *cyt c* under our experimental conditions. By fitting the data to equation XIII with a value of n = 2, the parameters of the adjustment are improved. The parameters for the second binding site show large error values of C_2 and b_2 but errors of k_2 are within acceptable limits. It is not demonstrated that ANS is unable to emit fluorescence when it is bound to an absorbed *cyt c* molecule. As in the case of blank samples, pure POPC and pure POPE show the highest and the lowest k_i values, respectively.

From the values of $\Delta\Psi$, it can be seen that the POPE:CL mixture (0.8:0.2, mol:mol) and pure CL show the greatest increase in surface potential due to *cyt c* adsorption, while POPE:POPC (0.6:0.4, mol:mol) shows the greatest decrease in $\Delta\Psi$. All samples containing *cyt c* show a decrease in fluorescence compared with blanks, which indicates that the protein is effectively adsorbed. In other words, negative values do not indicate that *cyt c* is not absorbed, but can instead be interpreted as an indication that *cyt c* can be adsorbed deeply in the liposome, probably due to hydrophobic forces. In these cases, the values of $\Delta\Psi$ cannot be completely accurate, because this mathematical procedure only takes into account the superficially adsorbed *cyt c*. Pure POPC shows high values of k_i and only moderate increases in $\Delta\Psi$ of 1.5 mV. In pure POPC liposomes, as with the compositions with negative $\Delta\Psi$ values, *cyt c* can be adsorbed deeply in the liposome, but in pure POPC there are enough protein molecules at the liposome surface to produce a positive variation in the value of $\Delta\Psi$. By contrast, pure POPE liposomes show the lowest k_i values but an increase in $\Delta\Psi$ of 7.5 mV. This large increase in the value of $\Delta\Psi$ when compared with pure POPC or the ternary mixture is caused by the fact that all *cyt c* molecules are located on the surface of the liposome, while in compositions containing POPC the proteins can be adsorbed in other locations.

Interestingly, the only mixed composition containing CL that shows a significant increase in the value of $\Delta\Psi$ is the POPE:CL (0.8:0.2, mol:mol). POPC:CL (0.6:0.4, mol:mol) and POPE:POPC:CL (0.5:0.3:0.2, mol:mol:mol) show an absolute variation in $\Delta\Psi$ of ~ 1 mV, while POPE:CL (0.8:0.2, mol:mol) shows an increase of almost 14 mV. This difference in *cyt c* adsorption suggests that an event occurs at the surface of POPE and CL liposomes that favours the adsorption of *cyt c*. It is worth noting here that the isotherm analysis performed in section V.1.1.3. reveals a phase separation of both molecules at $\chi_{CL} \sim 0.05$. Therefore, it is plausible that a certain degree of lateral segregation can appear in POPE:CL (0.8:0.2, mol:mol) liposomes. If this is the case, two lipid structures exist in the liposomes: one mainly composed of POPE and other mainly composed of CL. Since *cyt c* binds specifically to anionic molecules, the negative surface charge generated by the segregation of CL molecules is conducive to the adsorption of more *cyt c* molecules to these liposomes than in other compositions. Moreover, *cyt c* can bind to the region composed mainly of POPE, which then increases the value of $\Delta\Psi$.

To confirm the hypothesis that the specific adsorption of *cyt c* is caused by lipid segregation in POPE:CL (0.8:0.2, mol:mol) liposomes and not by the surface charge, new experimental strategies were adopted. In experiments with POPC:POPG (0.43:0.57, mol:mol) and POPE:POPG (0.66:0.33, mol:mol), the observed increases in the value of $\Delta\Psi$ are similar, but they are three times smaller than those observed for the POPE:CL (0.8:0.2, mol:mol) mixture. This indicates that the value of $\Delta\Psi$ induced by *cyt c* adsorption in POPE:CL (0.8:0.2, mol:mol) liposomes is not only dependent on the surface charge of CL molecules. Consequently, a specific organization of molecules in this composition can also contribute to the binding of *cyt c* molecules.

VI.4. AFM SPB CHARACTERIZATION

Since its invention, the AFM [Binning et al., 1986] has become as a fundamental tool in the characterization of biological samples below the micrometric scale with the added advantage of allowing observations under biomimetic conditions. This is the case in the

observation of bacteria and membranes and in the characterization and manipulation of proteins and DNA [Dufrene and Lee, 2000; Santos and Castanho, 2004].

The extension of liposomes over surfaces and the mechanism of rupture and transformation into planar structures – in this case supported planar bilayers, supported phospholipids bilayers or simply planar bilayers – has been extensively studied [Puu and Gustafson, 1997; Leonenko et al., 2004]. This study investigated the formation of SPBs with compositions that mimic the inner membrane of mitochondria with three purposes: (i) to explore the existence of segregated lipid domains with thermal or structural dependence; (ii) to corroborate the selective adsorption of *cyt c* to SPBs; and ultimately (iii) to determine the domain region dependence of this interaction.

The extension of the POPE:POPC (0.6:0.4, mol:mol) liposomes over mica creates SPBs with areas of more than 30 μm^2. Several defects can be seen. The SPB surface topography is smooth, without any distinctive feature irrespectively of the temperature at which the observation is made. Amplitude and phase images confirm that there are no changes when the temperature is increased. Note that the T_m value for liposomes of this composition is ~ 16 ºC, as observed from the midpoint of the fluorescence anisotropy experiments. As inferred from the thermodynamic analysis, since both lipids mix ideally at this molar ratio at the air-water interface, it is assumed that no domains or laterally segregated domains will be observed. The absence of thermal lipid domains is confirmed by the AFM images, which indicates that the AFM is a useful tool in demonstrating the presence or absence of these laterally segregated regions in model and natural membranes. It is important to mention that, in some cases, the substrate over which the liposomes are spread can modify the properties of the sample [Yang and Appleyard, 2000]. Alternatively, the lack of laterally segregated domains could be explained by differences in the molecular diffusion of the phospholipids, as a reflection of ideal mixing behaviour. Otherwise, due to the extremely soft nature of this sample, the AFM tip can compress the monolayers, thus reducing the height of the SPB and making it impossible to observe changes in the tilting orientation (estimated at less than 0.5 nm). By contrast, at 4 ºC the mobility of phospholipid molecules should be restricted, which would make the SPB more rigid. This would explain the differences in height at 4 ºC and 37 ºC. Other evidence of the increase in phospholipid lateral mobility

at 37 ºC can be inferred from the phase images. While at 4 ºC the mica and SPB surfaces show poor phase contrast (less than 3.5º), at 37 ºC this phase contrast is greater than 8º. At 4 ºC, phospholipid polar heads are closely packed, which produces an apparent hydrophilic SPB surface. At 37 ºC, due to the increase in the lateral mobility of the phospholipids, more exposed hydrophobic regions can interact with the AFM tip, which increases the phase contrast between the mica and SPB surfaces.

The extension of liposomes of POPC:CL (0.6:0.4, mol:mol) generates flat, round bilayers of ~ 3 μm in diameter. This composition does not form uniform lipid extensions but small, round SPBs of several micrometers in diameter. Similar behaviour has been observed for other phospholipid compositions [Merino et al., 2005b]. Close to the individual SPBs, small lipid extensions of ~ 200 nm in diameter appear that cannot be swept away or detached when the sample is rinsed with the free Ca^{2+} buffer. With greater sample incubation times, these small patches would tend to fuse with the SPB. The value of T_m for liposomes of this composition was determined as 4 ºC, by using the fluorescence anisotropy measurements for DPH. Therefore, the images at the lower observation temperature (4 ºC) are at exactly the T_m value of the sample. However, no phase separation was observed in either the topographic or the phase images. This could be because the AFM does not have sufficient resolution to observe topographic changes or alternatively because the solid support may modify the properties of the sample. Thus, we know that the value of T_m determined for SPBs is lower and the transition is broader than the values determined for liposomes [Leonenko et al., 2004]. The height differences of the SPB may be due to the increase in phospholipid lateral mobility as the temperature increases. In other words, at 4 ºC the SPB is higher than at 37 ºC. Interestingly, as can be seen in Figure 92D, the SPB topographic surface at 24 ºC shows less lateral cohesion that at 4 ºC or 37 ºC, because the AFM tip can effectively drag lipids away. This effect can be understood by examining the phase images for the same region. The phase images show several small protrusions on the SPB surface at temperatures below 25 ºC but none at 37 ºC. When the temperature is increased from 4 ºC to 24 ºC, the SPB incorporates these protrusions into its structure. This structural reorganization can modify the surface properties of the SPB and decrease its lateral stability. Moreover, small lipid structures near the SPB are destabilized at 37 ºC and the AFM tip drags them out of the scanning zone.

Numerous differences are observed between POPE:CL (0.8:0.2, mol:mol) samples in the presence or absence of calcium. The sample for the AFM observation was prepared by using the resuspension buffer containing Ca^{2+}. The DSC of the liposome suspension in the presence of the cation shows a sharp transition endotherm with a similar main transition to that observed in pure POPE. This suggests that a certain degree of lipid segregation occurs, which in turn means that pure lipid melting occurs.

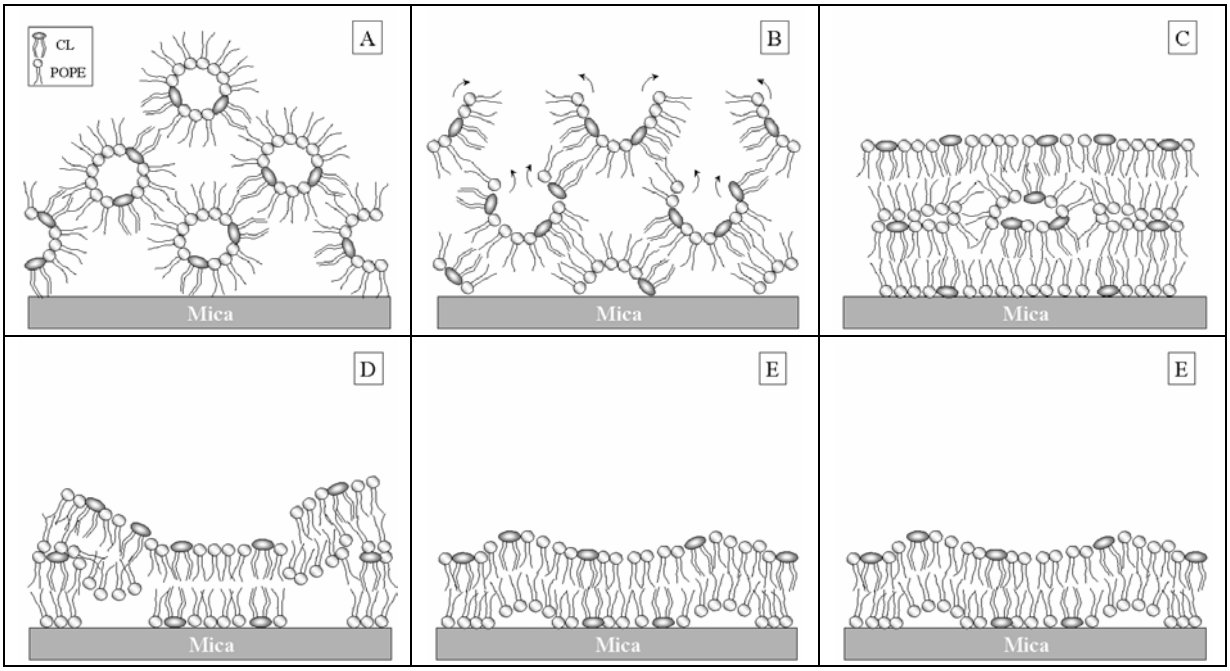

Figure 108. Schematic representation of the SPB formation from H_{II} structures in solution [Domènech et al., 2007].

Moreover, the ^{31}P-RMN power spectrum at 21 ºC (the temperature of sample formation) shows that the sample is mainly in the H_{II} phase [Epand and Bottega, 1988]. When the sample is incubated on the mica surface, the SPBs are not formed by vesicle fusion but by the fusion of inverted micelles [Domènech et al., 2007]. The hypothetical model for the formation of bilayers from H_{II} phases is shown in Figure 108.

The extension of lipid suspensions of POPE:CL (0.8:0.2, mol:mol) forms circular SPBs with mean diameters of ~ 50 μm. Each SPB is located no less than 300 μm from its nearest neighbour and no residual material can be found in the space between them. This could be due to a weak adsorption or attachment to the substrate, as can be deduced from the ease with which they are dragged away when the samples are rinsed

with a free Ca^{2+} buffer. However, the molecules in the SPB exhibit sufficient lateral stability to remain unaltered.

One of the most relevant observations made in this study is that the SPBs of this composition always show laterally, separated lipid domains within the range of temperatures assayed. At temperatures below 24 ºC, two domains can be clearly distinguished: the high domain and the intermediate domain, which have a step height difference of ~ 1.5 nm. At temperatures close to or above 24 ºC, the intermediate domain undergoes a transition while the high domain remains largely unaltered. Therefore, three lipid domains coexist at this temperature: the high, intermediate and low domains. The difference in height between the intermediate and low domains (~ 0.5 nm) can be attributed to a difference in the tilt angle of the species, asymmetric distribution or the formation of non-lamellar phases [Rainey and Skyes, 2005]. When the intermediate domain draws back from the edges of the SPB and the low domain appears, the high domain can diffuse against a more mobile, less stable domain, which increases its surface. At the initial stage, the high and intermediate domains are in equilibrium and the linear forces between domains are balanced. When the transition occurs in the intermediate domain due to the temperature increase, these forces are unbalanced and the high domain extends against or over the lower domain. Although the high domain covers a larger proportion of the SPB surface at 37 ºC than at 24 ºC, its height over the surface does not change substantially. Additionally, at 37 ºC the new high domain has the same bilayer thickness as observed at 24 ºC, while the low domain is 0.5 nm lower than the intermediate domain. The high domain is restricted to its initial area only when enclosed by the intermediate domain.

Interestingly, once the SPB is repeatedly scanned at a higher force, scratched areas are revealed on the high domain where material is swept away. These new areas have a similar height to the intermediate domain, which suggests that the material is in a fluid state, thus allowing a molecular reorganization of the SPB.

The ternary composition, POPE:POPC:CL (0.5:0.3:0.2, mol:mol:mol), forms large SPBs on the mica surface. These SPBs do not show any particular geometrical shape and do not cover all of the scanned area. Additionally, numerous small, circular

structures appear near the SPB that remain unaltered during the experiment. As can be seen from the topographic images (Figure 100), this SPB has a homogeneous, flat and featureless surface at 24 ºC. At this temperature the SPB shows one type of phospholipid structure, which is identified as the intermediate domain in section V.3.4. At 4 ºC two different structures can be seen on the surface of the SPB: a wide region of similar height to the intermediate domain at 24 ºC and a taller domain structured in isolated patches. These patches are not static; their shape and position changes in consecutive images taken at the same temperature. This indicates that the domains respond to temperature and appear or disappear due to friction caused by the AFM tip. Phospholipids in the taller domain will be in a gel state while phospholipids in the intermediate domain are in a more mobile state. The mobility of the phospholipid molecules causes the AFM tip record a lower measurement for the height of the SPB than when the phospholipids are in a more rigid state. No phase separation is shown between the two domains in the corresponding phase image, which demonstrates that both domains have the same composition. At 37 ºC two domains can again be seen on the SPB, but in this case its outline is poorly defined. At this temperature, the new lipid domain is shorter than intermediate domain visible at 24 ºC. As at 4 ºC, these lipid domains are not static and alter their shape after each successive scan. The appearance of this new lipid domain is caused by the transition of the molecules towards a more mobile state. No phase separation is observed in the phase image at 37 ºC, which indicates that the two domains have similar compositions.

Three different lipid domains are visible in the ternary mixture. The intermediate domain is present in the whole range of temperatures studied, but the high and low domains only appear at 4 ºC and 37 ºC, respectively. Another explanation for the appearance of the different domains could be that at 4 ºC, the SPB leaflet nearest to the mica surface is in a rigid state and only the outer SPB leaflet is in a more mobile state. As a result, the taller lipid domains in the outer leaflet of the SPB are in a more rigid state than the surrounding molecules. At 37 ºC, the entire outer SPB leaflet is in a mobile state and the new lipid domain could be created when part of the inner leaflet of the SPB melts. This effect can be seen in Figure 109.

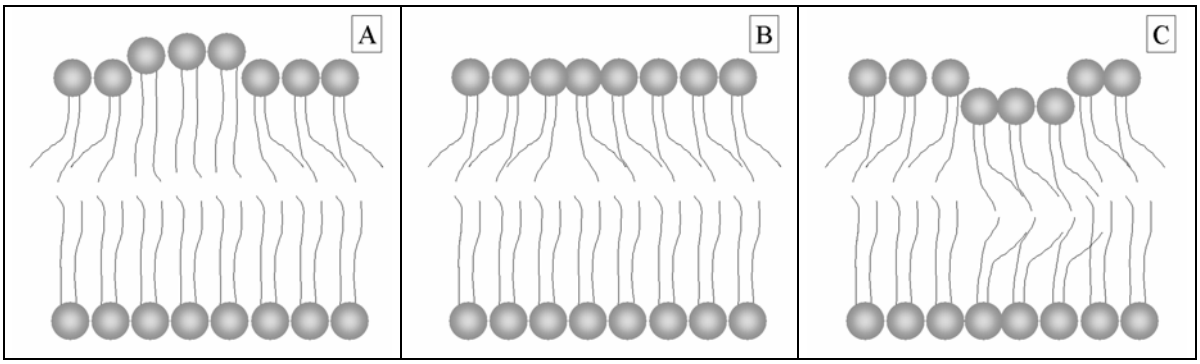

Figure 109. Schematic representation of an achievable process that could generate the three lipid domains in a ternary mixture A) 4 ºC, B) 24 ºC and C) 37 ºC.

If this hypothesis is certain, domains at 4 ºC might be clearly differentiated in the phase image. Unfortunately, in this experiment the phase images are contaminated with noise from interferences produced by the reflection of incident laser light on the substrate. This noise can distort the information from the phase image and make it impossible to distinguish the phase separation between domains.

VI.5. *IN SITU CYT C* INCORPORATION INTO SPBs

Cyt c is a peripheral protein located in the inner membrane of mitochondria. It is a small protein that is loosely attached to the membrane and has a main size of 6 x 6 nm^2 as identified by X-ray diffraction. Although *cyt c* is quite similar in size to the radius of the tip used with the atomic force microscope, smaller structures can be seen if they form repetitive structures.

The incorporation of *cyt c* into POPE:POPC (0.6:0.4, mol:mol) SPBs does not reveal individual *cyt c* molecules adsorbed onto the SPB surfaces. Besides, the incorporation of *cyt c* into the sample produces a decrease in the height of the SPB and a concomitant increase in its roughness value. This change in SPB height suggests that *cyt c* proteins could be adsorbed in a more internal location, which destabilizes the SPB surface and prevents the AFM tip from differentiating between *cyt c* and the SPB surface. SPB roughness increases after *cyt c* incorporation because adsorbed proteins alter the SPB surface profile. The measure of SPB height after *cyt c* incorporation could be inaccurate if some protein aggregates are adsorbed onto the mica surface, which would alter the value of the step height measured through section analysis. The phase images do not show new structures after *cyt c* incorporation on either the mica or the SPB surface, so

the variation in phase contrast between the two surfaces could be due to the fact that *cyt c* molecules are only adsorbed to the SPB surface but in deeper positions, thus modifying its viscoelastic properties.

Cyt c incorporation into POPC:CL (0.6:0.4, mol:mol) SPBs displays different behaviour to its incorporation into POPE:POPC (0.6:0.4, mol:mol) SPBs. In this case, *cyt c* molecules exert a lytic action on SPB surface that solubilizes part of it. This SPB rupture could be due to the fact that *cyt c* molecules are not adsorbed onto the SPB surface but instead penetrate into the SPB. If the surface local *cyt c* concentration is high enough, the *cyt c* molecules can perforate the SPB and solubilize part of it. After *cyt c* incorporation into the sample, a large number of small round structures appear on the SPB surface in the topographic and amplitude images. The phase image shows that almost all of the aggregates show a similar phase contrast to the SPB surface, which indicates that they are lipid aggregates. Only a few of these aggregates show a different phase contrast to the SPB surface, which proves that they are not lipid aggregates. These round structures appear in the image highlighted by a white rectangle. We know they are *cyt c* aggregates because they are larger than individual *cyt c* molecules.

It would be appropriate to recall here that the SPBs of POPE:CL (0.8:0.2, mol:mol) show lipid segregation at any temperature assayed. Therefore, the incorporation of *cyt c* into the different lipid domains could be performed in different ways. When *cyt c* is injected into the liquid cell it can form protein aggregates linked to the SPB surface, mainly at the edges of the high lipid domain. Such behaviour can be understood if we assume that at the boundary of lipid domains the interfacial tension decreases, thus accommodating the protein aggregates better than in the lipid domains themselves [van den Brink-van der Laan et al., 2004]. Nevertheless, the binding between these aggregates and the SPB is weak and the lateral displacement of the AFM tip can sweep the entities away from the edges of the high lipid domain.

More interesting it is the binding of *cyt c* to SPBs of POPE:CL (0.8:0.2, mol:mol), which is observed as a monomeric form. In the topographic image before *cyt c* injection, the high domain shows a roughness value of 0.13 nm, while after *cyt c* incorporation the same value is doubled (*Ra* = 0.29 nm), which indicates that proteins have been adsorbed

onto the surface. By contrast, there is no variation in the roughness values of the intermediate and low domains after *cyt c* injection. It is surprising that the phase contrast (from the colour scale) between the high lipid domain and the other two lipid domains is inverted after the incorporation of *cyt c* into the sample, which suggests that *cyt c* is only bound to the high lipid domain. An extended image of the high lipid domain reveals the presence of a large number of small, cylindrical structures of very similar size. This suggests that these structures could be individual molecules of *cyt c* adsorbed into the high lipid domain.

The surface of SPBs of POPE:POPC:CL (0.5:0.3:0.2, mol:mol:mol) shows two lipid domains before *cyt c* incorporation, which is consistent with the thermal response of this composition observed in the results section. Although the lipid domains are clearly distinguishable in the topography image, they do not appear as clearly in the phase images. In any case, the mica surface shows a difference phase contrast to the SPB surface, as can be seen from the colour scale. After *cyt c* is incorporated into the sample through the AFM liquid cell, small structures can be seen to appear on the SPB surface. The taller lipid domain that appears before the incorporation of *cyt c* is no longer present and a shorter lipid domain appears on the SPB surface, while the intermediate domain remains unaltered. These small structures can be identified as lipid aggregates as the phase image shows a similar phase contrast to SPB surface, which indicates that they have similar viscoelastic properties to the SPB. It is important to emphasize here that the difference in phase contrast between the SPB and mica surfaces after the incorporation of *cyt c* is less than the difference observed before the incorporation of the protein. The weak phase contrast might be due to the incorporation of the protein into only one of the two surfaces. This suggests that the protein can be incorporated into the SPB surface in such a way that it cannot be detected by the AFM tip in a monomolecular form, because the roughness value of the SPB surface increases for more than that of the mica surface